

Calculated elastic constants and anisotropy of Mg_2SiO_4 spinel at high pressure

Boris Kiefer¹ and Lars Stixrude¹

School of Earth and Atmospheric Sciences, Georgia Institute of Technology

Renata M. Wentzcovitch

Dept. of Chemical Engineering and Materials Science, University of Minnesota

Abstract. We calculated the elastic properties of Mg_2SiO_4 spinel, using the plane-wave pseudopotential method. The athermal elastic constants were calculated directly from the stress-strain relations up to 30 GPa, which encompasses the experimentally observed stability field of spinel. The calculated elastic constants are in very good agreement with Brillouin scattering data at zero pressure. We calculated the isotropically averaged elastic wave velocities and the anisotropy from our single crystal elastic constants. We find that the elastic anisotropy is weak (azimuthal and polarization anisotropy of S-waves: 5%, azimuthal P-wave anisotropy: 2.5%, at zero pressure) compared to other silicates and oxides. The anisotropy decreases initially with increasing pressure, changing sign at 17 GPa before increasing in magnitude at higher pressures. At typical pressures of the earth's transition zone (20-25 GPa), the elastic anisotropy is 1% and 2% for P- and S-waves respectively.

Introduction

The elasticity of Mg_2SiO_4 spinel (ringwoodite) is of considerable geophysical interest for a number of reasons: spinel is thought to be the most abundant mineral in the lower part of the transition zone (520-660 km depth) and its elastic properties will play an important role for our understanding of the composition of this region [Ita and Stixrude, 1992].

Another important issue is the elastic anisotropy of this mineral at high pressures. Analyses of seismological observations of anisotropy in terms of mantle flow are primarily based on elastic constants measured at zero pressure [Karato, 1997; Fischer and Wiens, 1996; Montagner and Kennett, 1996]: the elastic constants of spinel have only been measured at ambient conditions [Weidner *et al.*, 1984] and the pressure dependence of the elastic constants and the anisotropy remain completely unknown. Isotropic averaged velocities have been measured below 3 GPa [Rigden *et al.*, 1992].

To address these issues, we have determined the structure, the equation of state and the elastic constants of

spinel up to 30 GPa which encompasses the experimentally observed stability field of spinel. From the elastic constants we determine the seismic wave velocities and the single crystal anisotropy for spinel for the first time at high pressure.

Computational Methods

To obtain the ground state properties of spinel at arbitrary pressures, we use a method that combines density functional theory and molecular dynamics with variable cell shape [Wentzcovitch *et al.*, 1995]. Density functional theory provides in principle an exact formalism for the ground state density and energy of an electronic system. Our method makes two essential approximations: (1) the electrons are treated in the local density approximation (LDA); (2) The pseudopotential approximation. This method has been applied successfully to a wide variety of systems including silicates and oxides [Wentzcovitch *et al.*, 1995; Karki *et al.*, 1997].

We used norm-conserving pseudopotentials [Troullier *et al.*, 1991]. For silicon and oxygen we used the same pseudopotentials as in previous calculations [daSilva *et al.*, 1997]. For magnesium we used a new pseudopotential which treats the Mg 2p electrons as valence electrons. The motivation was given by previous LAPW calculations on MgO where the Mg 2p electrons were treated as semi-core states [Mehl and Cohen, 1988]. The magnesium pseudopotential we used gives very good agreement between our predicted structures and experiments for periclase and spinel. Our results underestimate the zero pressure volumes and bondlength for both structures by $\approx 3\%$ and $\approx 1\%$ respectively. Some of this error is attributed to LDA. The Brillouin zone was sampled on a 2x2x2 Monkhorst-Pack grid, the planewave cutoff was chosen to be 80Ry, leading to 37500 planewaves per Mg_2SiO_4 unit.

To determine the elastic constants we first determined the equilibrium structure at each pressure. The unit cell of the relaxed structure was then subjected to a chosen strain and re-optimized. We used a single (monoclinic) strain to calculate the three elastic constants c_{11} , c_{12} and c_{44} . We applied positive and negative strains (magnitude 1%) in order to determine accurately the stresses in the appropriate limit of zero strain. Similar variable cell shape methods have been used to calculate elastic constants for earth materials like periclase [Karki *et al.*, 1997]. In all cases the agreement between experiment and theory was favorable.

¹Now at Department of Geological Sciences, University of Michigan, Ann Arbor, Michigan.

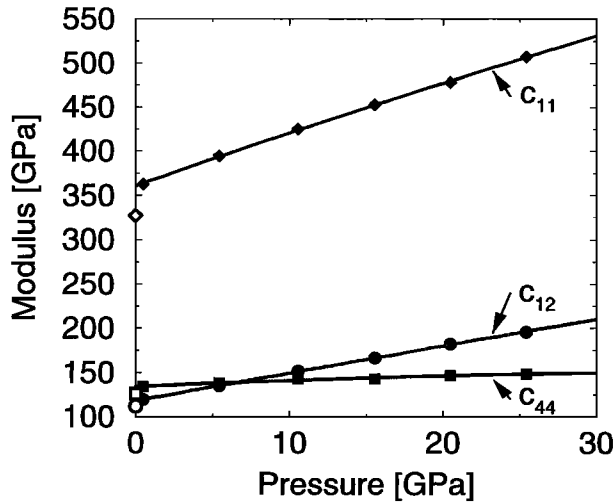


Figure 1. Computed elastic constants of Mg_2SiO_4 spinel. Filled symbols are theoretical results, solid lines are Eulerian finite strain fits with the parameters given in Table 1. Experimental results from *Weidner et al.*, 1984, are shown as open symbols.

Results

We calculated the pressure dependencies of the three elastic constants c_{11} , c_{12} and c_{44} up to 30 GPa. Our elastic constants agree favorably with available experimental Brillouin scattering data at zero pressure [*Weidner et al.*, 1984]. The athermal elastic constants are systematically larger than those determined by experiment (largest deviation: 9% for c_{11}). Deviations of several percent are expected due to the experimental temperature (300K). The remaining discrepancies between theory and experiment are attributed to the LDA. The elastic constants depend sub-linearly on pressure over the whole pressure range. The pressure dependence of the elastic constants was represented by a third order expansion in the Eulerian finite strain [*Davies*, 1974] (Fig. 1 and Table 1).

We calculated the isotropic averaged velocities for compressional (P) waves and shear (S) waves in the *Hashin-Shtrikman* [1962] scheme to compare our result to ultrasonic measurements below 3 GPa [*Rigden et al.*, 1992] and to the velocity structure of the lower part of the transition zone (Fig. 2). The velocities determined from our athermal elastic constants are higher than those of room temperature experiments (P-wave: by 5%, S-wave: 2%). We used the measured temperature dependence of the elastic constants for MgAl_2O_4 spinel to estimate the temperature effect (Table 1).

The pressure derivatives of the wave velocities we find are smaller than those derived from ultrasonic experiments [*Rigden et al.*, 1992] (Table 1). We speculate that this difference may be due to the porosity of the samples at low pressures, the small pressure range (1.5 GPa) of the ultrasonic experiments. Moreover, we note that our calculated value of K'_0 agrees with subsequent equation of state measurements [*Meng et al.*, 1994].

In order to address the issue of the pressure dependence of elastic anisotropy in spinel, we calculated the directional dependence of the P- and the S-wave velocity by solving the Christoffel equation. P-wave velocities are extremal for propagation along [111] and [100]. The shear wave polarized in (001) (S1) is extremal along [100] and [110]. The shear wave polarized in (110) (S2) is extremal along $[1/2, 1/2, 1/\sqrt{2}]$ and [100].

As a measure of single crystal anisotropy in cubic crystals we use (*Karki et al.*; [1997]):

$$A_X = \frac{M_X[\vec{n}_0] - M_X[100]}{c_{11}} \quad (1)$$

where \vec{n}_0 is the extremal propagation direction other than [100], $X \in \{P, S1, S2\}$, and M_X is the modulus corresponding to the wave velocity $M_X = \rho V_X^2$. From the Christoffel equation it can be shown that this measure of anisotropy for the three acoustic waves can be cast into a single parameter [*Karki et al.*, 1997]:

$$A = \frac{2c_{44} + c_{12}}{c_{11}} - 1 \quad (2)$$

Table 1. Comparison of elastic moduli, M_0 , their pressure derivatives M'_0 , elastic wave velocities and their pressure derivatives (in $\text{km s}^{-1} \text{GPa}^{-1}$) as determined from theory and experiment.

	Theory		Experiment	
	$M_0(\text{GPa})$	M'_0	$M_0(\text{GPa})^1$	$M'_0(-)^2$
c_{11}	361 (348)	6.32	327	-
c_{12}	118 (112)	3.18	112	-
c_{44}	134 (129)	0.82	126	-
K	199 (190)	4.19	184	4.99, 4.2
μ	129 (125)	1.12	119	1.73
V_P (km s^{-1})	10.08 (9.93)	0.052	9.79	0.078
V_S (km s^{-1})	5.94 (5.87)	0.010	5.77	0.025

References: 1, Brillouin scattering data *Weidner et al.* [1984]; 2, ultrasonic measurements *Rigden et al.* [1992], except for the second value listed for K'_0 from *Meng et al.* [1994]. Theoretical values are from a third order finite strain fit to the first principles results. Bulk and shear moduli are Hashin-Shtrikman averages calculated from the elastic constants. The values for K_0 and K'_0 are consistent with the values derived from the equation of state $V_0 = 512.6 \text{ \AA}^3$, $K_0 = 196.0 \text{ GPa}$ and $K'_0 = 4.34$. Values in parentheses give the elastic constants at 300K, the temperature dependence is taken from measurements in the MgAl_2O_4 system [*Cynn*, 1992]. Experimental values of K and μ are determined as Voigt-Reuss-Hill averages.

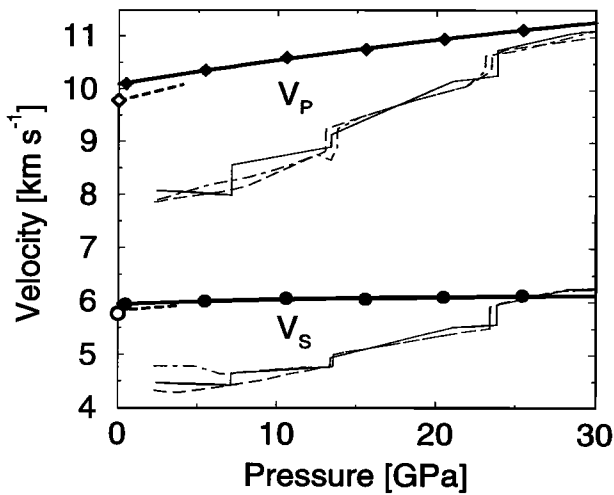


Figure 2. Hashin-Shtrikman average velocities determined from our theoretical elastic constants (filled diamonds and filled circles) compared with ultrasonic measurements [Rigden *et al.*, 1992, thick dashed lines]; Brillouin spectroscopy data [Weidner *et al.*, 1984, open symbols]; P-wave seismological models GCA [Walck, 1984, thin long-dashed line] and CJF [Walck, 1985, thin short-dashed line]; S-wave models TNA and GNA [Grand and Helmberger, 1984, thin long-dashed and thin short-dashed line respectively]; the values from PREM [Dziewonski and Anderson [1981]] are shown as thin solid lines.

The anisotropy defined in (1) is then given by:

$$A_P = \frac{2}{3}A, \quad A_{S1} = -\frac{1}{2}A, \quad A_{S2} = -\frac{3}{8}A. \quad (3)$$

The pressure dependences of the parameter A is shown in Fig. 3. In addition we calculated the polarization and azimuthal anisotropy for S-waves and the azimuthal anisotropy for P-waves, defined by:

$$\Delta_{S,polarization} = \frac{\max\{|V_{S1}[\vec{n}] - V_{S2}[\vec{n}]|\}}{V_{S,aggregate}} \quad (4)$$

$$\Delta_{S,azimuthal} = \frac{|\{V_{S1}[\vec{n}_0]\} - \{V_{S2}[100]\}|}{V_{S,aggregate}} \quad (5)$$

$$\Delta_{P,azimuthal} = \frac{|\{V_P[\vec{n}_0]\} - \{V_P[100]\}|}{V_{P,aggregate}} \quad (6)$$

The pressure dependence of these measures are shown in Fig. 3. For cubic systems, S-wave azimuthal and polarization anisotropy coincide.

The anisotropy decreases initially with increasing pressure, at 17 GPa spinel is elastically isotropic. For higher pressures, the anisotropy changes sign and increases in magnitude. This behavior can be understood in terms of the direction of the extremal wave velocities. At low pressures, the P-wave is fastest along [111] direction (A positive), at higher pressure the fast P-wave direction is [100] (A negative). The change of sign of A also explains why S2 waves are fastest at low pressure but S1 waves are fastest at high pressure and also the behavior shown by the polarization and azimuthal anisotropy.

We found that the single crystal elastic anisotropy of Mg_2SiO_4 spinel is small (Fig. 3) in contrast to the

anisotropy in forsterite [daSilva *et al.*, 1997]. At typical pressure conditions for the lower part of the transition zone (20-25 GPa) the anisotropy is 1% and 2% for P- and S-wave anisotropy respectively.

Geophysical Implications

A comparison of the pressure dependence of our calculated isotropic P- and S-wave velocities with the velocity structure for the lower part of the transition zone, shows that the velocity profiles are almost parallel and that the calculated values are shifted to higher values by 8% and 9% for P- and S- waves respectively. The differences can be accounted for by the presence of iron, which lower the velocities by $\approx 2-3\%$ and the high temperatures in this depth range which decrease the velocities by $\approx 8\%$ relative to the athermal values [Weidner *et al.*, 1984]. Other abundant minerals in the transition zone like majorite and Ca-perovskite may also contribute to this difference.

The relatively weak anisotropy of spinel found here contrasts with the global seismological study of Montagner and Kennett, [1996], who find a transverse anisotropy in the lower part of the transition zone of 2-4%. The anisotropy due to an aggregate of spinel at transition zone pressures may be a factor 5 less than that observed, based on our results and assuming typical polycrystalline textures [Karato, 1997]. Moreover this difference cannot be accounted for by the presence of iron or high temperatures in the mantle [Cynn, 1992; Wang and Simmons, 1972]. An iron content of 11% is expected to raise the elastic anisotropy by 1% while transition zone temperatures increase the anisotropy by 1% and 3% for P- and S-waves respectively. Accounting for the effect of iron and temperature, our results are consistent with the observations of Fischer and Wiens, [1996] who find an upper bound of 0.5% for transverse S-anisotropy in the transition zone below the Tonga subduction zone.

Models that interpret observations of anisotropy in terms of mantle flow rely primarily on the measured elastic constants at zero pressure. However elastic anisotropy can show a complex pressure dependence as in

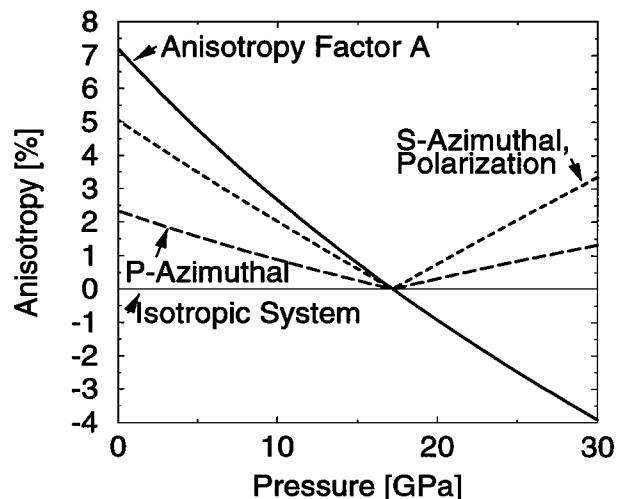


Figure 3. Computed anisotropy factor A (solid line), S-wave polarization anisotropy and S-wave azimuthal anisotropy (short dashed line), P-wave azimuthal anisotropy (long dashed line).

periclase [Karki *et al.*, 1997] or spinel. The magnitude of the elastic anisotropy of spinel is small in the whole pressure range from 0 to 30 GPa, but it changes sign at 17 GPa. This shows that the zero pressure anisotropy is not necessarily representative of the elastic anisotropy at high pressures as in the lower part of the transition zone.

Acknowledgments. This work was supported by the National Science Foundation under grants EAR-9628199 (LPS) and EAR-9628042 (RMW), and by the Minnesota Supercomputer Institute.

References

- Cynn, H., Effects on cation disordering in $MgAl_2O_4$ spinel on the rectangular parallelepiped resonance and Raman measurements of vibrational spectra, Ph.D. thesis, 169pp, UCLA, Los Angeles, November 1992.
- Davies, G. F., Effective elastic moduli under hydrostatic stress - I. quasiharmonic theory, *Journal of the Physics and Chemistry of Solids*, 35, 1513-1520, 1974.
- Dziewonski, A. M., and D. L. Anderson, Preliminary reference Earth model, *Physics of the Earth and Planetary Interiors*, 25, 297-356, 1981.
- Fischer, K. M., and D. A. Wiens, The depth distribution of mantle anisotropy beneath the Tonga subduction zone, *Earth and Planetary Science Letters*, 142, 253-260, 1996.
- Grand, S. P., and D. V. Helmberger, Upper mantle shear structure of North America, *Geophys. J. R. astr. Soc.*, 76, 399-438, 1984.
- Hashin, Z., and S. Shtrikman, A variational approach to the theory of the elastic behavior of polycrystals, *Journal of Mechanics and Physics of Solids*, 10, 343-352, 1962.
- Ita, J., and L. Stixrude, Petrology, Elasticity, and Composition of the Mantle Transition Zone, *J. Geophys. Res.*, 97, 6849-6866, 1992.
- Karato, S., Seismic Anisotropy in the Deep Mantle, Boundary Layers and the Geometry of Mantle Convection, in *Geodynamics of the Lithosphere and the Earth's Mantle* (edited by J. Plomerova, V.N. Babuska, and R.C. Liebermann), submitted.
- Karki, B. B., L. Stixrude, S. J. Clark, M. C. Warren, G. J. Ackland, and J. Crain, Structure and elasticity of MgO at high pressure. *American Mineralogist*, 82, 52-61, 1997.
- Mehl, M. J., and R. E. Cohen, Linear Augmented Plane Wave electronic structure calculations for MgO and CaO, *Journal of Geophysical Research*, 93, 8009-8022, 1988.
- Meng, Y., Y. Fei, D. J. Weidner, G. D. Gwanmesia, and J. Hu, Hydrostatic Compression of γ - Mg_2SiO_4 to Mantle Pressures and 700K: Thermal Equation of State and Related Thermoelastic Properties, *Phys. Chem. Minerals*, 21, 407-412, 1994.
- Montagner, J. P., and B. L. N. Kennett, How to reconcile body-wave and normal mode-reference earth models, *Geophys. J. Int.*, 125, 229-248, 1996.
- Ridgen, S. M., G.D. Gwanmesia, I. Jackson, and R. C. Lieberman, progress in high-pressure ultrasonic interferometry, the pressure dependence of elasticity of Mg_2SiO_4 polymorphs and constraints on the composition of the transition zone of the earth's mantle, *High-Pressure Research: Application to Earth and Planetary Sciences*, edited by Syono, Y. and M. H. Manghani, 167-182, 1992.
- daSilva, C., L. Stixrude, and R. M. Wentzcovitch, Elastic Constants and Anisotropy of Fosterite at High Pressure, *Geophysical Research Letters*, 24, 1963-1966, 1997.
- Troullier, N., and J. L. Martins, Efficient pseudopotentials for plane-wave calculations. *Physical Review B*, 43, 1993-2003, 1991.
- Walck, M. C., The P-wave upper mantle structure beneath an active spreading center: The Gulf of California, *Geophys. J. R. astr. Soc.*, 76, 697-723, 1984.
- Walck, M. C., The upper mantle beneath the north-east Pacific rim: a comparison with the Gulf of California, *Geophys. J. R. astr. Soc.*, 81, 243-276, 1985.
- Wang, H., and G. Simmons, Elasticity of some mantle crystal structures 1. Pleonaste and hercynite spinel, *J. Geophys. Res.*, 77, 4379-4392, 1972.
- Weidner, D. J., H. Sawamoto, and S. Sasaki, Single-crystal elastic properties of the spinel phase of Mg_2SiO_4 , *Journal of Geophysical Research*, 89(B9), 7852-7860, 1984.
- Wentzcovitch, R. M., N. L. Ross, and G. D. Price, Ab initio study of $MgSiO_3$ and $CaSiO_3$ perovskite at lower mantle pressures, *Phys. Earth Planet. Int.*, 90, 101-112, 1995.

Boris Kiefer and L. Stixrude, Department of Geological Sciences, University of Michigan, Ann Arbor, MI 48109.

R. M. Wentzcovitch, Dept. of Chemical Engineering and Materials Science, University of Minnesota, Minneapolis, MN 55455.

(Received May 28, 1997; accepted August 29, 1997.)